TECHNOLOGIE 5G

Bulletin de veille scientifique : Juillet 2025

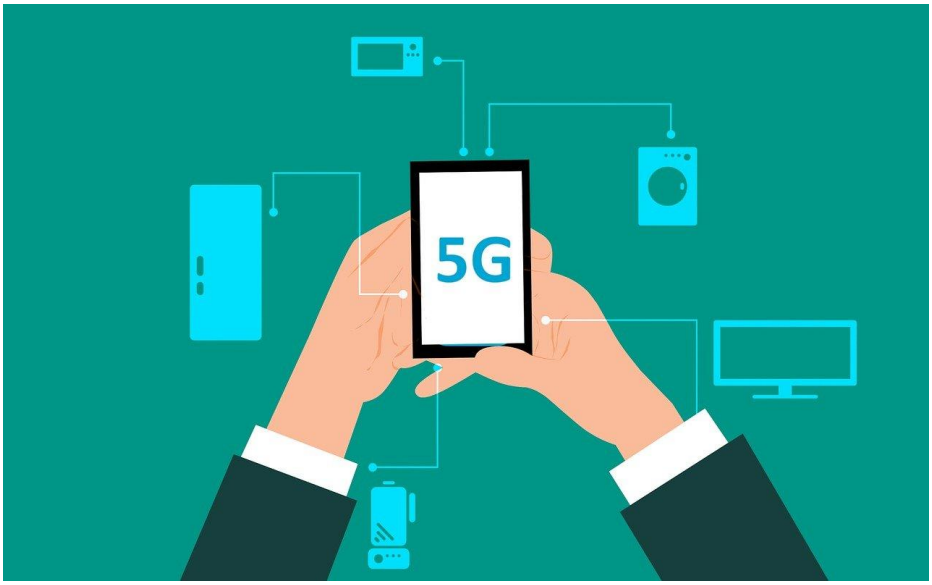

Objectifs : réaliser une veille scientifique sur la technologie 5G

La validation des informations fournies (exactitude, fiabilité, pertinence par rapport aux principes de prévention, etc.) est du ressort des auteurs des articles signalés dans la veille. Les informations ne sont pas le reflet de la position de l'INRS. Les éléments issus de cette veille sont founis sans garantie d'exhaustivité. Les liens mentionnés dans le bulletin donnent accès aux documents sous réserve d'un abonnement à la ressource.

Les bulletins de veille sont disponibles sur le portail documentaire de l'INRS. L'abonnement permet de recevoir une alerte mail lors de la publication d'un nouveau bulletin (bouton « M'abonner » disponible après connexion à son compte).

Généralités

Aucun article dans ce bulletin.

Antennes

Miniaturized Dual and Quad Port MIMO Antenna Variants Featuring Elevated Diversity Performance for UWB and 5G-Midband Applications.

Ramanathan K, Gopalakrishnan S, Chandrakanthan T. *Micromachines (Basel)*. 2025 Jun 17;16(6).

The growing demand for high-speed and high-capacity wireless communication has intensified the need for compact, wideband, and efficient MIMO antenna systems, particularly for 5G mid-band and UWB applications. This article presents a miniaturized dual and quad port MIMO antenna design optimized for 5G mid-band (n77/n78/n79/n96/n102) and Ultra-Wideband (UWB) applications without employing any decoupling structures between the radiating elements. The 2-port configuration features two closely spaced symmetric monopole elements (spacing < λ(max)/2), promoting efficient use of space without degrading performance. An FR4 substrate (εr = 4.4) is used for fabrication with a compact size of 30 × 41 × 1.6 mm(3). This layout is extended orthogonally and symmetrically to form a compact quad-port variant with dimensions of 60 × 41 × 1.6 mm(3). Both designs offer a broad operational bandwidth from 2.6 GHz to 10.8 GHz (8.2 GHz), retaining return loss (S(XX)) below -10 dB and strong isolation (S(XY) < -20 dB at high frequencies, <-15 dB at low frequencies). The proposed MIMO antennas demonstrate strong performance and excellent diversity characteristics. The two-port antenna achieves an average envelope correlation coefficient (ECC) of 0.00204, diversity gain (DG) of 9.98 dB, and a mean effective gain difference (MEG(ij)) of 0.3 dB, with a total active reflection coefficient (TARC) below -10 dB and signal delay variation under 0.25 ns, ensuring minimal pulse distortion. Similarly, the four-port design reports an average ECC of 0.01432, DG of 9.65 dB, MEG(ij) difference below 0.3 dB, and TARC below -10 dB, confirming robust diversity and MIMO performance across both configurations.

Lien vers l'article

Metamaterial based tri-band compact MIMO antenna system for 5G IoT applications with machine learning performance verification.

Rahman MA, Al-Bawri SS, Larguech S, Alharbi SS, Alsowail S, Jizat NM, et al. *Sci Rep*. 2025 Jul 2;15(1):22866.

This paper presents a novel tri-band Multiple Input Multiple Output (MIMO) antenna module designed for millimeter and microwave frequency bands, employing metamaterial (MTM) technology to enhance performance. The compact antenna module measures 36 × 36 × 1.6 mm(2) and uses a Rogers RT-5880 substrate. Its structure includes a multi-stubbed radiating patch, a partial ground plane, and a 2 × 1 epsilon-negative MTM array positioned between antenna elements in an orthogonal layout. Operating at 3.5 GHz, 5.2 GHz, and 28 GHz, the integration of MTM significantly improves the antenna's overall performance by influencing phase, amplitude, and electromagnetic field distribution. Bandwidth enhancements of 10.01% and 6.4% are achieved for the 3.5 GHz and 5.2 GHz microwave bands, respectively, and 4.43% for the 28 GHz millimeter-wave band. Isolation levels improved from 20 dB to 24 dB in microwave bands and from 26 dB to 32 dB in the millimeter-wave band, ensuring reduced interference. The realized gain also increased from 3.6 dBi, 4.2 dBi, and 7.4 dBi to 4.8 dBi, 5.3 dBi, and 9.3 dBi across the respective frequency bands. The proposed MIMO antenna showcases excellent diversity performance with an envelope correlation coefficient (ECC) of below

0.002/0.001/0.0003 across all bands and a diversity gain (DG) exceeding 9.98 dB. Machine learning-based performance verification analysis assessed bandwidth and efficiency, where the K-Nearest Neighbors (KNN) model achieved 97.8% accuracy. This MIMO antenna holds great potential for various Internet of Things (IoT) applications, including Vehicle-to-Network, Vehicle-to-Cloud communications, 5G cellular networks, Wi-Fi, WiMAX, and both sub-6 GHz and millimeter-wave 5G bands, reinforcing its suitability for 5G IoT sectors.

Lien vers l'article

A compact single layer dual-polarized antenna with wideband operation, high isolation, and high front-to-back ratio for 5G applications.

Hussain N, Tran H, Tran-Huy D, Kim-Thi P. *Sci Rep*. 2025 Jul 15;15(1):25613.

This paper proposed a simple design of dual-polarized antenna with a single layer and compact structure for 5G applications. The proposed antenna performs several advantages of wideband, high isolation, as well as high front-to-back ratio characteristics. Instead of using complicated feeding network or stacked structure, a directed-fed crossed patch antenna is employed. Noted that by locating the feeding locations close to the center, high isolation can be achieved without requiring any complicated feeding scheme. Additionally, four parasitic patches are introduced to not only enhance the operating bandwidth but also improve the front-to-back ratio. The final antenna with compact overall dimensions of 0.46λ × 0.46λ × 0.02λ exhibits wideband operation of 7.5% (4.76-5.13 GHz) and high isolation of better than 23 dB. Besides, despite having compact size, the antenna achieves a broadside gain of about 6.0 dB and the front-to-back ratios of around 15 dB across the operating bandwidth.

Lien vers l'article

High-isolation dual-band MIMO antenna for next-generation 5G wireless networks at 28/38 GHz with machine learning-based gain prediction.

Haque MA, Ananta RA, Ahammed MS, Nirob JH, Sawaran Singh NS, Paul LC, et al. *Sci Rep*. 2025 Jul 1;15(1):20782.

This research outlines the results on implementing a Machine Learning (ML) approach to improve the throughput of Multiple-Input Multiple-Output (MIMO) based 5G millimeter wave applications. The research will cover frequencies between 28 and 38 GHz, significantly affecting high-band 5G applications. We have chosen to employ a Rogers RT 5880 material with a low loss as the substrate layer to reduce the antenna size. In addition to being small, the recommended design has a maximum gain of 10.14 dB, better isolation than 29 dB, and wide bandwidth, ranging from 27.2 GHz to 32.2 GHz & 36.5 GHz to 40.7 GHz. Advanced design system (ADS) is used to make a circuit like the suggested microstrip patch antenna (MPA) to compare the reflection coefficient from CST. The approach of supervised regression machine learning is applied to accurately forecast the antenna's gain. Among the five different regression machine learning models considered, it was discovered that the Random Forest Regression (RFR) model performed the best in accuracy and achieved the lowest error when predicting gain. This article explores many approaches, including simulation, integration of an RLC-equivalent circuit model, and multiple regression models, to evaluate the suitability of an antenna for its 5G applications.

Lien vers l'article

Miniaturization of Sub 6 GHZ Band 5G Monopole Antenna with Manganese Assisted CoFe(2)O(4) Nano Self-Assembly Magneto-Dielectric Coating.

Dayanidhi V, Krishnan T, Dheivasigamani T. *ACS Omega*. 2025 Jun 24;10(24):26041-51.

This paper proposes a miniaturized monopole antenna for sub-6 GHz 5G mobile applications by integrating a magneto-dielectric superstrate. The Magneto dielectric material is composed of manganese-assisted CoFe(2)O(4) ferrite-based nanoself-assembly materials. The Gel Matrix method is utilized to synthesize MnFe(2)O(4), CoFe(2)O(4), and Mn-doped CoFe(2)O(4) magneto-dielectric ferrite nanoparticles. Structural and morphological analysis of the synthesized particles is conducted using X-ray diffraction (XRD) and scanning electron microscopy (SEM). The magneto-dielectric (MDL) coating over the antenna is done by mixing the ferrite powders with polyvinylidene fluoride (PVDF) polymer. The effects of the magneto dielectric layer on the monopole antenna's performance are assessed in terms of return loss, radiation pattern, and impedance bandwidth using a vector network analyzer and an Anechoic Chamber. A significant improvement in the impedance bandwidth (400 MHz) is observed for the Mn-doped CoFe(2)O(4)-PVDF coating, achieving a bandwidth of 3.00 to 3.4 GHz. The antenna exhibits miniaturization with a resonance frequency shift to 3.2 GHz, achieving a peak gain of 2.6 dBi. The results demonstrate that the Mn-doped CoFe(2)O(4)-PVDF superstrate effectively supports antenna miniaturization for the sub-6 GHz frequency bands, such as n77 and n78, used in 5G applications.

Lien vers l'article

Array inspired wideband and high gain antenna with enhanced pattern diversity for 5G mm wave networks.

Alqwaifly NA, Awan WA, Alsaab N, Alsunaydih FN, Alhassoon K. *Sci Rep*. 2025 Jul 28;15(1):27383.

This paper presents a four-port MIMO antenna array designed for future 5G millimeter-wave applications. Initially, a single antenna element is developed by loading two semi-circular stubs onto a basic rectangular patch to enhance the impedance bandwidth. To further improve the antenna's performance, a three-element array is designed and optimized for high-performance characteristics. Subsequently, the array is extended to a four-element MIMO configuration for diverse applications. The proposed antenna system is designed and analyzed using Rogers TMM-4 substrate with a thickness of 1.52 mm. This substrate is selected due to its low loss and dielectric properties similar to those of FR-4. The performance of all three antenna designs is evaluated in terms of S-parameters, gain versus frequency, radiation patterns, and radiation efficiency. Additionally, MIMO performance parameters are studied for the MIMO antenna configuration. The proposed antennas operate in the millimeter-wave frequency band ranging from 24.4 to 27.9 GHz. Beyond return loss and operational bandwidth, the array also offers high gain, and the investigation of MIMO performance metrics demonstrates excellent characteristics. To verify and validate the simulated results, hardware prototypes of both the standalone and array antennas are fabricated and measured. The measured results show good agreement with the simulated data. Finally, the performance of the proposed antenna is compared with recently published work. The results and comparison confirm that the proposed antenna features a compact size and simple structural configuration, while offering wide bandwidth, high gain, and acceptable MIMO parameter values. These attributes make the proposed antenna a strong candidate for integration into upcoming 5G devices operating in the millimeter-wave spectrum.

Lien vers l'article

Compact Frequency-Agile and Mode-Reconfigurable Antenna for C-Band, Sub-6-GHz-5G, and ISM Applications.

Ali EM, Awan WA, Abbas A, Abbas SM, Mohamed HG. *Micromachines (Basel)*. 2025 Jun 19;16(6).

This article presents the design and evaluation of a compact-sized antenna targeting heterogenous applications working in the C-band, 5G-sub-6GHz, and the ISM band. The antenna offers frequency reconfigurability along with multi-operational modes ranging from wideband to dual-band and tri-band. A compact-sized antenna is designed initially to cover a broad bandwidth that ranges from 4 GHz to 7 GHz. Afterwards, various multiband antennas are formed by loading various stubs. Finally, the wideband antenna along with multi-stub loaded antennas are combined to form a single antenna. Furthermore, PIN diodes are loaded between the main radiator and stubs to activate the stubs on demand, which consequently generates various operational modes. The last stage of the design is optimization, which helps in achieving the desired bandwidths. The optimized antenna works in the wideband mode covering the C-band, Wi-Fi 6E, and the ISM band. Meanwhile, the multiband modes offer the additional coverage of the LTE, LTE 4G, ISM lower band, and GSM band. The various performance parameters are studied and compared with measured results to show the performance stability of the proposed reconfigurable antenna. In addition, an in-depth literature review along with comparison with proposed antenna is performed to show its potential for targeted applications. The utilization of FR4 as a substrate of the antenna along with its compact size of 15 mm × 20 mm while having multiband and multi-mode frequency reconfigurability makes it a strong candidate for present as well as for future smart devices and electronics.

Lien vers l'article

Performances et sécurité

5G Network Slicing: Security Challenges, Attack Vectors, and Mitigation Approaches.

Dias J, Pinto P, Santos R, Malta S. *Sensors (Basel)*. 2025 Jun 24;25(13).

This paper explores the security challenges associated with network slicing in 5th Generation (5G) networks, a technology that enables the creation of virtual networks tailored to different use cases. This study contributes to network slicing research efforts by providing a comprehensive classification of attacks aligned with the architectural layers of 5G, complemented by practical mitigation approaches suitable for multi-tenant environments. The classification depicts specific attacks and categorizes vulnerabilities across layers such as orchestration, virtualization, and inter-slice communication. Additionally, mitigation strategies are discussed, emphasizing the importance of real-time monitoring and robust access controls. The proposed classification aims to support the development of advanced security mechanisms, including risk assessment models and automated mitigation strategies, tailored to the dynamic and heterogeneous nature of 5G slicing. The findings highlight the need for layered defenses, AI-driven monitoring, and architectural isolation as critical components to enhance the resilience of 5G slicing deployments.

Lien vers l'article

Enhanced spectrum sensing for 5G and LTE signals using advanced deep learning models and hyperparameter tuning.

Elmorsy SMA, Osman SM, Gamel SA. *Sci Rep*. 2025 Jul 10;15(1):24825.

This paper introduces a novel approach to enhancing spectrum sensing accuracy for 5G and LTE signals using advanced deep learning models, with a particular focus on the impact of systematic hyperparameter tuning. By leveraging state-of-the-art neural network architecture, namely DenseNet121 and InceptionV3-the study aims to overcome the limitations of traditional spectrum sensing methods in highly dynamic and noisy wireless environments. The research highlights that, through rigorous hyperparameter optimization, these models achieved substantial improvements in detection accuracy, reaching 97.3% and 98.2%, respectively, compared to initial performance levels of 93.0% and 95.0%. These performance improvements were particularly notable in controlled scenarios where low signal-to-noise ratio frames were excluded, with 60% of frames containing little or no information-highlighting the critical role of signal quality in both training and evaluation. It is worth noting that the models were trained and tested on a large and diverse dataset, including synthetic signals and real-world data, simulating a wide range of practical deployment conditions. This comprehensive database supports the generalizability of the proposed approach and its real-world applicability. The study also confirms that the models demonstrated competitive performance in various test scenarios, and that their integration into future wireless systems could significantly enhance smart spectrum management and real-time communication reliability in modern networks.

Lien vers l'article

Effect of elevation on cumulative radiofrequency exposure from multiple communication towers.

Osei S, Quarshie E, Azah CK, Fuseini AR, Dogbey R, Deatanyah P, et al. *Radiat Prot Dosimetry*. 2025 Jul 24;201(10):701-8.

A densely populated place like a public university needs good internet and communication connectivity for effective academic work. As such, University campuses in Ghana are inundated with communication antennas. This study investigated how radiofrequency (RF) power density levels are affected by the elevations of different floors of high-rise buildings of a public university. A spectrum analyser coupled to a log-periodic antenna was used. The RF power density decreased from the ground floor to the third floor and only increased to maximum levels on the fourth floor. The variation across different floors indicates the influence of elevation on the measured EMF levels. The 900 MHz band produced the highest power density of 1.16E-03 W/m2 on the last (fourth) floor, suggesting that communication applications in the 900 MHz band are the most used by the university community.

Lien vers l'article

A Fault-Tolerant Localization Method for 5G/INS Based on Variational Bayesian Strong Tracking Fusion Filtering with Multilevel Fault Detection.

Deng Z, Ma Z, Luo H, Guo J, Tian Z. *Sensors (Basel)*. 2025 Jun 16;25(12).

In this paper, for the needs of high-precision and high-continuity localization in complex environments, a modeling method based on time-varying noise and outlier noise is proposed, and variational Bayesian strong tracking filtering is used for 5G/INS fusion localization. A hierarchical progressive fault detection mechanism is proposed to detect IMU rationality faults and consistency faults in 5G observation

information. The main contributions are reflected in the following two aspects: first, by innovatively introducing Pearson VII-type distribution for noise modeling, dynamically adjusting the tail thickness characteristics of the probability density function through its shape parameter, and effectively capturing the distribution law of extreme values in the observation data. Afterward, this article combined the variational Bayesian strong tracking filtering algorithm to construct a robust state estimation framework, significantly improving the localization accuracy and continuity in non-Gaussian noise environments. Second, a hierarchical progressive fault detection mechanism is designed. A wavelet fault detection method based on a hierarchical voting mechanism is adopted for IMU data to extract the abrupt features of the observed data and quickly identify faults. In addition, a dual-channel consistency detection model with dynamic fault-tolerant management was constructed. Sudden and gradual faults were quickly detected through a dual-channel pre-check, and then, the fault source was identified through AIME. Based on the fault source detection results, corresponding compensation mechanisms were adopted to achieve robust continuous localization.

Lien vers l'article

Deep learning for enhancing automatic classification of M-PSK and M-QAM waveform signals dedicated to single-relay cooperative MIMO 5G systems.

Chikha HB, Alaerjan A, Jabeur R. *Sci Rep*. 2025 Jul 18;15(1):26018.

Automatic modulation classification (AMC) is a critical component in modern communication systems, particularly within software-defined radios, cognitive radio networks, smart grid and and distributed renewable energy systems (RESs) where adaptive and efficient signal processing is essential. This paper proposes a novel deep learning-based AMC method for identifying M-PSK and M-QAM waveform signals in single-relay cooperative MIMO 5G systems operating under partial channel state information (CSI) and spatially correlated channels. The proposed method leverages a convolutional neural network (CNN) classifier trained on a reduced set of discriminative features, including higher-order statistics and the differential nonlinear phase peak factor, which are extracted from the received signal. Feature dimensionality is reduced using the Gram-Schmidt orthogonalization procedure to enhance training efficiency. A centralized decision-making strategy aggregates predictions from multiple antennas. The method is evaluated through simulations using various modulation orders and under challenging conditions such as low signal-to-noise ratios (SNR). Results demonstrate that the proposed CNN-based approach significantly outperforms benchmark machine learning classifiers in terms of classification accuracy, precision, recall, and F-measure. These findings underscore the practical potential of the method for enhancing AMC performance in realistic 5G cooperative scenarios.

Lien vers l'article

Architecture réseau

An enhanced performance analysis of load based resource sharing framework for MIMO systems in 5G communication systems.

Logeshwaran J, Patel SK, Kumar OP, Al-Zahrani FA. *Sci Rep*. 2025 Jul 2;15(1):23327.

Resource sharing serves as a cost-effective and dynamically adjustable method for alleviating traffic congestion in wireless networks. Advancements in multi-input multi-output (MIMO) technologies for

5G communication systems have led to the exploration of resource sharing across various cells or sectors. This approach aims to optimise network performance, focussing on coverage, capacity, and quality of service. This document presents a new load-based resource-sharing framework designed for multi-cell MIMO systems. The proposed framework utilises channel-loading data from local base stations and dynamically allocates available resources among adjacent base stations. The proposed framework facilitates dynamic resource sharing, effectively addressing traffic overload in 5G networks. The proposed LBRS achieved a delta-P value of 90.91%, a prevalence threshold value of 89.84%, a critical success index value of 91.01%, and a Mathew's correlation coefficient value of 91.27% at the terminal access. At the resource transmission, the system recorded a delta-P value of 92.10%, a prevalence threshold value of 92.18%, a critical success index value of 91.65%, and a Mathew's correlation coefficient value of 88.31%. The simulation results indicate that the proposed framework effectively enhances dynamic resource sharing, resulting in a notable improvement in network performance.

Lien vers l'article

Efficacité énergétique

How Beyond-5G and 6G Makes IIoT and the Smart Grid Green-A Survey.

Varga P, Jászberényi Á I, Pásztor D, Nagy B, Nasar M, Raisz D. *Sensors (Basel)*. 2025 Jul 6;25(13).

The convergence of next-generation wireless communication technologies and modern energy infrastructure presents a promising path toward sustainable and intelligent systems. This survey explores how beyond-5G and 6G communication technologies can support the greening of Industrial Internet of Things (IIoT) systems and smart grids. It highlights the critical challenges in achieving energy efficiency, interoperability, and real-time responsiveness across different domains. The paper reviews key enablers such as LPWAN, wake-up radios, mobile edge computing, and energy harvesting techniques for green IoT, as well as optimization strategies for 5G/6G networks and data center operations. Furthermore, it examines the role of 5G in enabling reliable, ultra-low-latency data communication for advanced smart grid applications, such as distributed generation, precise load control, and intelligent feeder automation. Through a structured analysis of recent advances and open research problems, the paper aims to identify essential directions for future research and development in building energy-efficient, resilient, and scalable smart infrastructures powered by intelligent wireless networks.

Lien vers l'article

Autres équipements

Novel high-performance microstrip diplexer for 5G mid-band and wide-band applications: Design, analysis and manufacturing.

Yahya SI, Zubir F, Abdel Hafez M, Nouri L, Chaudhary MA, Assaad M, et al. *PLoS One*. 2025;20(7):e0327839.

This paper presents the design and experimental results of a microstrip diplexer with a high performance for 5G applications. The introduced diplexer has compact size, novel structure, low

losses, and wide fractional bandwidth. Notably, it exhibits a novel microstrip layout with a very compact size of 0.004 λg2. The resonance frequencies are tuned at 1.1 GHz and 3.2 GHz for mid-band 5G applications. The presented structure has the fractional bandwidths (57.3%, 44.6%) and insertion losses (0.07 dB, 0.04 dB). Additionally, it features two flat channels with two low maximum group delays of 0.86 ns, 0.4 ns in the 1st and 2nd passbands, respectively. A perfect mathematical design method is applied to find the behavior of the introduced resonator, as well as the most effective physical dimensions. For improving the performance and miniaturization, an optimization method is used. To validate the design approach, the proposed diplexer is fabricated and then measured, demonstrating a close agreement between the simulation and measurement results. This highlights the effectiveness of our design approach and underscores the potential of the proposed diplexer for enabling efficient and reliable communication in the rapidly evolving field of telecommunications.

Lien vers l'article

Applications industrielles

Aucun article dans ce bulletin.

Applications médicales

Exploring the emerging trends and hot topics of 5G technology application in wireless medicine: A bibliometric and visualization analysis.

He Y, Xie J, Weng Z, Yang F, Wei Y, Liang J, et al. *Medicine (Baltimore)*. 2025 Jul 18;104(29):e43310.

BACKGROUND: The online diagnosis and treatment model based on 5th generation mobile communication (5G) technology is one of the important ways to solve the imbalance between supply and demand of medical services. OBJECTIVE: We systematically summarized Chinese and English literature on the application of 5G technology in the field of wireless medical and conducted a literature feature analysis. METHODS: We used bibliometrics to quantitatively analyze the research trends and hot topics and comparatively analyzed the differences between research in China and other countries. RESULTS: This study analyzed 1344 articles and found that China provided the most funding (531 [75.32%]) and far outnumbered other countries in this field (1014 vs 330), but the quality of articles and effective collaboration between authors need to be improved. The hot topics in this field have gradually shifted from the construction of 5G internet hospitals during the COVID-19 to the construction of smart hospitals based on the Internet of Medical Things, and the research focus has gradually shifted from the data transmission layer such as wearable devices to the application layer of smart medical services. CONCLUSION: Researchers can further refine the specific application of 5G technology in the field of wireless medical from the 3 major areas of the smart hospital system.

Lien vers l'article

5G-remote radical prostatectomy under novel robotic systems: a prospective comparative cohort study with local surgeries.

Ye S, Peng D, Zhu L, Zhu Y, He A, Jing T, et al. *Prostate Cancer Prostatic Dis*. 2025 Jul 28.

BACKGROUND: There is no report upon the remote surgery of radical prostatectomy and comparisons between local surgeries. This study aims to evaluate the feasibility and safety of the innovative remote tele-surgical robotic platforms in performing radical prostatectomy. METHODS: The study comprised 13 patients diagnosed with prostate cancer who underwent remote radical prostatectomy using a 5 G wireless network and the innovative remote robotic systems (Tele-RARP). Additionally, the research involved 31 patients who underwent radical prostatectomy with the local Toumai robotic system (TM-RARP) between October 2022 and April 2024, and 36 patients who underwent radical prostatectomy with the da Vinci Xi platform (Xi-RARP) during the same period under the supervision of the same surgical team. Data on demographics, perioperative factors, clinicopathologic information, and postoperative results were collected for a total of 80 patients. RESULTS: The completion of 13 Tele-RARP procedures was successful without significant intraoperative or postoperative issues. No

instances of intraoperative blood transfusion or surgical conversion were reported. The operation, console, and docking time for both the remote and local surgeries showed minimal differences. Neither local nor remote surgery nor da Vinci Xi surgery exhibited significant variations in terms of blood loss, intraoperative complications, or postoperative prognosis. Both TM-RARP and Tele-RARP presented very manageable task loads. CONCLUSIONS: Performing tele-surgical robotic-assisted radical prostatectomy using the innovative Toumai and Edge robotic surgical systems via a 5 G wireless network is not only feasible but also safe. REGISTRATION NUMBER: ChiCTR2400085386, ChiCTR2300077721.

Lien vers l'article

A pilot experience on 5G telerobotic long-distance magnetic navigation-guided ablation for cardiac arrhythmias.

Liu Z, Bao Y, Lin C, Li X, Wei Y, Luo Q, et al. *Europace*. 2025 Jul 1;27(7).

Lien vers l'article

Evaluation (Mesure des niveaux d'exposition)

Méthodes d'évaluation

Aucun article dans ce bulletin.

Evaluation population générale

In-Situ Measurements of Radiofrequency Electromagnetic Fields Measurements Around 5G Macro Base Stations in the UK.

Calderon C, Addison D, Peyman A. *Bioelectromagnetics*. 2025 Jul;46(5):e70012.

Radiofrequency (RF) electromagnetic field spot measurements were performed in line-of-sight to 56 active 5G macro base stations across 30 publicly accessible locations in the United Kingdom (UK). Four different exposure scenarios were assessed: background (no traffic instigation), streaming videos, downlink speed test, and extrapolation of SS-RSRP decoder measurements. Power density measurements across the 420 MHz-6 GHz frequency range were also performed at each site to assess the total exposure from various RF sources in the environment. Both total RF and 5G specific power density levels were found to be well within the 1998 ICNIRP public reference levels, even when extrapolating to worst-case scenario (≤ 5%). 4G downlink was the dominant contributor to total RF exposure, with 5G contributing on average less than 10%. No statistically significant difference was observed between beamforming and non-beamforming sites. Streaming did not seem to contribute materially to exposure levels, suggesting that background measurements are a good representation of typical downlink exposure at current urban and suburban 5G sites.

Lien vers l'article

Risques professionnels

Aucun article dans ce bulletin.

In silico

Aucun article dans ce bulletin.

In vitro

Exposure to 26.5 GHz, 5G modulated and unmodulated signal, does not affect key cellular endpoints of human neuroblastoma cells.

Sannino A, Allocca M, Scarfì MR, Romeo S, Peluso V, Panariello G, et al. *Sci Rep*. 2025 Jul 1;15(1):20614.

The fifth generation (5G) network is currently being worldwide spread out, raising questions about its potential health impact. The current study aimed to investigate the effects of a 26.5 GHz 5G electromagnetic field on key cellular endpoints of human neuroblastoma cells. A reverberation chamber-based exposure system was designed and realized which allowed the exposure/sham exposure of cell cultures under highly controlled exposure conditions of both electromagnetic and biological parameters. The suitability of the reverberation chambers to host cell cultures was verified by evaluating cell proliferation and cell cycle progression. The effect of 3 h exposure at specific absorption rate of 1.25 W/kg under both continuous wave and 5G modulated signal was evaluated in terms of cell cycle and DNA damage. In the latter case, the exposure was also given in combination with menadione to account for possible cooperative effects. Results showed absence of effects of exposure given alone and in combination with menadione, when both continuous wave and modulated signals were applied at the mentioned exposure level. Further investigations are needed by varying the exposure and biological parameters to strengthen the absence of effects due to 5G signals in the range of millimeter waves.

Lien vers l'article

Impact of Radiofrequency Electromagnetic Fields on Cardiac Activity at Rest: A Systematic Review of Healthy Human Studies.

Michelant L, Selmaoui B. *Bioelectromagnetics*. 2025 Jul;46(5):e70014.

Radiofrequency electromagnetic fields (RF-EMF) exposure is increasingly prevalent, raising concerns about potential non-thermal health effects. This systematic review synthesizes current evidence regarding RF exposure effects on cardiac activity, focusing on heart rate (HR) and heart rate variability (HRV). Studies on healthy individuals were selected based on strict methodological criteria, including experimental design, control for confounding variables, and sufficient details on exposure parameters. Articles were included if they compared healthy subjects with and without exposure and provided cardiac measurements, specific absorption rate, or exposure measurement. A total of 28 articles were analyzed. This review included studies with RF exposure ranging from 100 to 110,000 MHz and exposure durations varying from short periods to 7 nights, with most studies lasting between 5 and 50 min. Most studies demonstrated no significant effects of RF exposure on HR, regardless of the exposure system, frequency, duration, age, sex, distance, or subject position. Findings for HRV were

more nuanced, with most studies indicating no significant impact on key HRV parameters. However, some position-dependent variations emerged, particularly in antenna-based studies. Additionally, our analysis suggests that RF exposure may particularly interfere with cardiac regulatory mechanisms when the cardiovascular system is challenged and required to adapt, such as during postural changes or physiological maneuvers, although there are insufficient comparable studies to validate this hypothesis. Importantly, all included studies were conducted under resting or non-stressful conditions and involved only healthy participants. Therefore, our conclusions cannot be generalized to stressed states or clinical populations. Moreover, methodological harmonization is needed to improve comparability across future studies. The main limitation of the current evidence being the heterogeneity of experimental protocols, highlighting the need for methodological standardization in future studies. To address current heterogeneity, we propose specific methodological recommendations, including systematic blinding, accurate exposure measurement and detailed exposure, to improve comparability and reproducibility in future studies. Bioelectromagnetics. 00:00-00, 2025. © 2025 Bioelectromagnetics Society.

Lien vers l'article

Sur l'animal

Research on the Correlation between BDNF Val76Met Polymorphism and Susceptibility to Changes of Cognitive Function in Rats Induced by Microwave Radiation.

Zhang M, Wang Y, Zou Y, Zhi W, Zhao X, Niu J, et al. *Neurochem Res*. 2025 Jul 19;50(4):238.

Microwave radiation is extremely sensitive to the brain and has been shown in animal models to affect memory and learning. Brain-derived neurotrophic factor (BDNF) is essential for neural function and brain development, with many single nucleotide polymorphisms (SNPs) in gene. Several neuropathological disorders have been linked to the BDNF Val66Met variation. Using CRISPR, we created BDNF Val76Met mutations in rats in this study. The rats were then subjected to X-band and S-band microwave radiation, respectively, at an average power density of 50 mW/cm² for 15 min every day for five days. We assessed cognitive capacity and investigated the neural structure and BDNF mRNA levels in the brain of rats. We discovered that BDNF Val76Met rats had impaired learning capacity and altered brain structure, with a decrease in BDNF mRNA. Meanwhile, we found that BDNF Val76Met rats exhibited aggravated structural and functional brain damage under 50mW/cm(2) microwave radiation, and showed higher sensitivity to S-band microwave due to the stronger penetration compared to X-band microwaves. Considering the genetic differences between animals and humans, more research is needed to determine the exact mechanism by which this SNP location affects cognitive changes caused by microwave radiation.

Lien vers l'article

Histological and inflammatory effects of 26.5 GHz quasi-millimeter wave exposure on rat skin.

Ijima E, Nagai A, Li K, Hikage T, Kamizawa N, Hidaka E, et al. *Front Public Health*. 2025;13:1580155.

INTRODUCTION: Information regarding the biological effects of localized exposure to quasi-millimeter waves (qMMW) is limited. Given that qMMW exposure can elevate skin temperature and potentially induce thermal injury, further investigation is required. In this study, we aimed to evaluate histological changes and the expression of inflammation-related markers in rat skin tissue locally exposed to

26.5 GHz qMMW, as well as investigate the threshold for inflammatory responses. METHODS: The dorsal skin of rats was locally exposed to 26.5 GHz qMMW at absorbed power densities (APD) of 0, 250, 370, and 500 W/m(2) for 18 min using a patch antenna. Histological changes and expression patterns of inflammation-related markers were examined in skin tissue sections exposed to qMMW. Furthermore, serum levels of prostaglandin E(2) (PGE(2)), tumor necrosis factor-α (TNF-α), and interleukin-6 (IL-6) were measured at each post-exposure time point. RESULTS: Histological analysis revealed burn-like tissue damage in the 500 W/m(2) exposure group, characterized by subepidermal blister formation, epidermal thickening, and dermal edema, which increased in severity over time. Conversely, the lower exposure groups (250 and 370 W/m(2)) showed no distinct morphological changes, similar to the sham group. The 500 W/m(2) group exhibited significantly elevated expression of inducible nitric oxide synthase (iNOS) and ionized calcium-binding adapter molecule 1 (Iba1), particularly in the dermis, dermal white adipose tissue, and sebaceous glands. Serum levels of PGE(2) increased in a dose-dependent manner at 24 and 72 h; TNF-α and IL-6 remained undetectable. The skin temperature increased during qMMW exposure, reaching 39.0 ± 0.6°C, 42.4 ± 0.9°C, and 44.8 ± 1.2°C at APDs of 250, 370, and 500 W/m(2), respectively. DISCUSSION: Localized exposure of rat skin to qMMW induces burn-like tissue degeneration and triggers an inflammatory response. This effect may be thermally induced by qMMW irradiation, with the threshold estimated to range between 370 and 500 W/m(2) APD under the present experimental conditions. Few studies have demonstrated MMW-induced inflammatory responses in the skin. To the best of our knowledge, this is the first study to clearly define the threshold using APD as a reference. These findings may contribute useful evidence for future revisions of exposure guidelines.

Lien vers l'article

Characterization of the Core Temperature Response of Free-Moving Rats to 1.95 GHz Electromagnetic Fields.

Bala N, Croft RJ, McIntosh RL, Iskra S, Frankland JV, McKenzie RJ, et al. *Bioelectromagnetics*. 2025 Jul;46(5):e70013.

The present study investigated the core body temperature (CBT) response of free-moving adult male and female Sprague Dawley rats, during and following a 3-h exposure to 1.95 GHz radiofrequency electromagnetic fields (RF-EMFs) within custom-built reverberation chambers, using temperature capsules implanted within the intraperitoneal cavity and data transmitted via radiotelemetry. Comparing RF-EMF exposures (at Whole-Body Average-Specific Absorption Rate [WBA-SAR] levels of 0.1, 0.4, and 4 W/kg) to the sham exposed condition, we identified a statistically significant peak increase in CBT after 26 min of RF-EMF exposure at 4 W/kg (+0.49°C), but not in the 0.1 or 0.4 W/kg conditions at the same timepoint. In the last 30 min of the RF-EMF exposure, temperature was significantly increased in both the 4 W/kg (0.62°C) and 0.4 W/kg (0.14°C) conditions, but not 0.1 W/kg, when compared to sham. After 20 min following cessation of exposure, post temperature was still significantly higher in the 4 W/kg condition when compared to the sham (0.37°C), but not in either 0.1 or 0.4 W/kg. Based on our findings, it is apparent that rats can effectively compensate for increased thermal loads of up to 4 W/kg as the maximum temperature rise was substantially lower than 1°C. In addition, the elevated CBT during exposure in the 4 W/kg condition was significantly reduced immediately after exposure cessation, indicating that measures of CBT following RF-EMF exposure cessation may not reflect maximum RF-EMF-mediated changes in the CBT of rats. Bioelectromagnetics. 00:00-00, 2025.

Lien vers l'article

Sur l'homme

Aucun article dans ce bulletin.

Reproduction

The effects of radiofrequency radiation on male reproductive health and potential mechanisms.

Bektas H, Dasdag S. *Electromagn Biol Med*. 2025;44(3):359-84.

Recent studies have demonstrated that radiofrequency (RF) radiation emanating from devices such as mobile phones and Wi-Fi may have adverse effects on male reproductive health. This radiation can elevate testicular temperature, potentially compromising sperm quality and DNA integrity, and influence the specific absorption rate (SAR) across different body regions, leading to detrimental reproductive outcomes. Furthermore, exposure to RF radiation has been linked to conditions that could affect male reproductive function, such as oxidative stress, alterations in ion transitions across cell membranes, and inflammation. The article reviews research conducted on both humans and animal models regarding the effects of electromagnetic radiation on sperm quality, DNA damage, oxidative stress, hormone levels, and testicular function, suggesting that exposure to electromagnetic radiation could have harmful implications for male reproductive health. However, further research is necessary to fully understand the mechanisms and implications of non-ionizing electromagnetic radiation on male infertility.

Lien vers l'article

Dispositifs médicaux implantables

Aucun article dans ce bulletin.